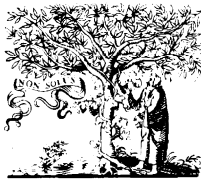


FATIGUE DESIGN OF COMPONENTS

Editors: G. Marquis and J. Solin

ESIS Publication 22

This volume represents a selection of papers presented at the Second International Symposium on Fatigue Design, FD' 95, held in Helsinki, Finland on 5–8 September, 1995. The meeting was organised by VTT Manufacturing Technology and co-sponsored by the European Structural Integrity Society (ESIS) and the American Society for Testing and Materials (ASTM). Partial funding for the event was provided by the Commission of the European Communities and City of Helsinki.



Elsevier

Amsterdam • Oxford • New York • Lausanne • Tokyo • Shannon

FRACTURE MECHANICAL FATIGUE ANALYSIS OF RAILWAY WHEELS WITH ROLLING DEFECTS

K.-O. Edel and G. Boudnitski
Fachhochschule Brandenburg
D-14770 Brandenburg an der Havel, Germany

ABSTRACT

Reusable solid railway wheels manufactured of the old wheel steel BV 1 (nearly equivalent to the solid or monobloc wheel steel R1 according to the new nomenclature) show in some cases rolling defects on the surface of the wheel disc. The fatigue behaviour of such defects is analysed by means of the linear-elastic fracture mechanics and Monte Carlo simulation and assessed to be able to derive the allowable defect size for the non-destructive testing.

KEYWORDS

fracture mechanics, fatigue, threshold ranges of the stress intensity factor, railway wheel, rolling defects, Monte Carlo simulation, safety factors, allowable defect size.

NOMENCLATURE

r	radial coordinate
r_{norm}	normal distributed random number with the mean 0 and the standard deviation 1
s_{ob}	standard deviation of the braking stresses in radial direction
s_{σ}	standard deviation of the residual stresses in radial direction
t_{rim}	thickness of the rim of the solid wheel
α	inclination angle between the crack area and the surface of the wheel disc
σ_{brake}	braking stress in radial direction
σ_{res}	residual stress in radial direction

INTRODUCTION

The rolling stock of the railways usually has a limited service life of some decades. At the end of their life the wagons will be scrapped. But not all parts of the railway structures will be unusable at this time. In many cases the wheels show only a very small wear on the tread so that the wheel sets are reusable.

At the reconditioning of the reusable wheel sets the wheels will be tested non destructively. Circumferentially and radially directed surface defects on the wheel disc were found in some cases. According to metallographic micro slices these defects are rolling defects with a finite or infinitely small tip radius.

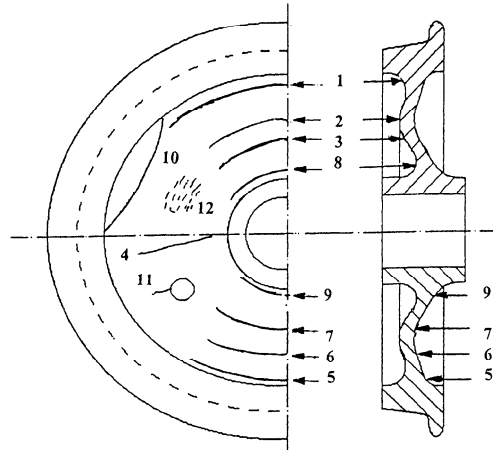


Fig. 1. The different kinds of rolling defects on the surface of the wheel disc.



Fig. 2. Micro slice transverse to the defect [1].

For the following investigations the rolling defects are assumed as cracklike defects with an infinitely small crack tip radius. Under this realistic assumption it is possible to use the linear elastic fracture mechanics to analyse and to assess the behaviour of these defects.

GEOMETRY OF DEFECTS

The tangentially directed defects which are of special interest show a length L of up to 600 mm. The inclined crack size a under the surface of the wheel disc has a size of up to about 10 mm. The correlation between the defect length L on the surface and the crack size a under the surface is given in Fig. 3.

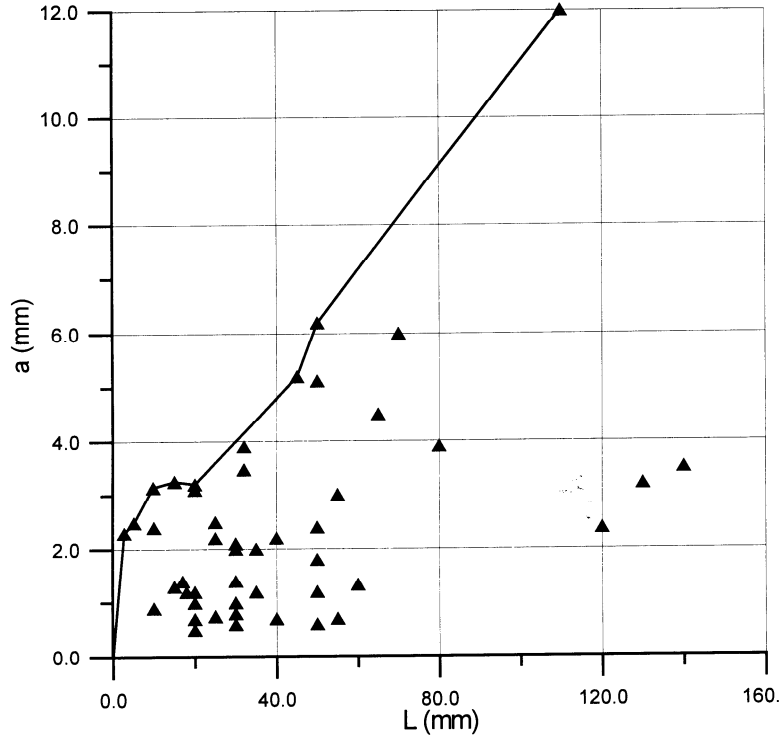


Fig. 3. Correlations between the inclined crack size a and the defect length L on the surface of the wheel disc.

The inclination of the crack area against the surface of the wheel disc lies between 0° and 90° with a mean value of about 25° . The probability of the inclination angle is approximated by the equation

$$P(\alpha) = 1 - \exp\left[-\left(\frac{\alpha - 8.46^\circ}{18.01^\circ}\right)^{1.11}\right]. \tag{1}$$

STRESSES AND STRESS INTENSITY FACTORS

Stresses in the Wheel Disc [2]

The wheel force components which act on the rim of the wheel depend on the track and rail geometry. The vertical wheel force component F_Q acts on the tread. It has a size of up to 170 kN for a load ca-

capacity of the wheel set of 20 tons. The horizontal wheel force component F_Y acts either on the flange ($F_Y > 0$) or on the inner side of the rim ($F_Y < 0$). It is scattered in the range of -23 up to 55 kN for the same load capacity.

The stresses in the wheel disc are measured under static conditions for predetermined wheel force components. The positioning of the strain gauges -in the 0°-position - were between the wheel set axle and the contact point with the rail. The stresses are given for the calculations by the equations

$$\sigma_{r,0^\circ} = c_Q \cdot F_Q + c_Y \cdot F_Y \quad \text{and} \quad \sigma_{r,180^\circ} = -c_Y \cdot F_Y. \quad (2)$$

Residual stresses in the disc of some solid wheels have been measured by means of strain gauges. Depending on the radius r of the position of the strain gauge, the residual stresses are approximated by the equation

$$\sigma_{res} = \sigma_{res}(r=0) + \frac{d\sigma_{res}}{dr} \cdot r + s_{cr} \cdot r_{norm} \quad (3)$$

with the regression coefficients given in Table 1. The radius r is limited to values between 171 mm and 317 mm corresponding to the extreme positions of the strain gauges.

Table 1. Coefficients for describing the residual stresses in solid wheels.

surface	$\sigma_{res}(r=0)$	$d\sigma_{res}/dr$	s_{cr}
outer	-218.45 MPa	0.7375 MPa/mm	80 MPa
inner	+249.59 MPa	-1.2484 MPa/mm	80 MPa

Thermal stresses in the disc of tread braked solid wheels have been calculated for a differently shaped wheel under usual stop brakings [3]. The thermal stresses are strongly influenced by the thickness of the rim of the wheel. For the calculation of the braking stresses in the disc the following rough approximation is used

$$\sigma_{brake} = \sigma_{brake}(t_{rim}=0) + \frac{d\sigma_{brake}}{dt_{rim}} \cdot t_{rim} + s_{ob} \cdot r_{norm}. \quad (4)$$

with the coefficients given in Table 2 and the thicknesses of the rim between 16 and 93 mm.

Table 2. Coefficients for describing the braking stresses in radial direction.

$\sigma_{brake}(t_{rim}=0)$	$d\sigma_{brake}/dt_{rim}$	s_{ob}
229.74 MPa	-1.2338 MPa/mm	22.4 MPa

Stress Intensity Factors

Solutions for the plane problem of straight inclined edge cracks loaded by constant tension (membrane stresses) and bending stresses are given in the handbook published by MURAKAMI [4]. The most complete solution of the mixed mode problem is given by BOWIE [5] for membrane stresses. The solutions to the equivalent bending problem show a reduction of the calibration factors of up to 50 per cent for the same nominal stresses.

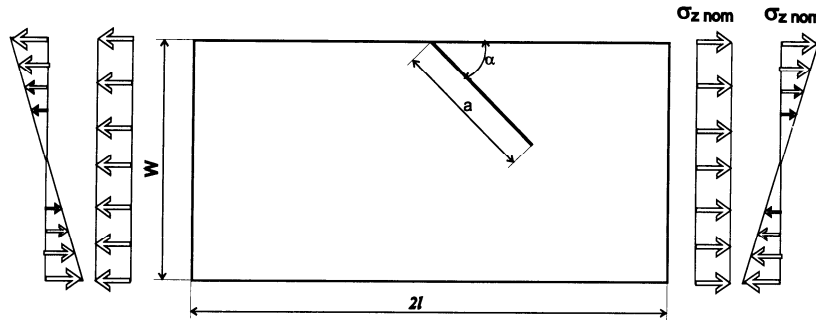


Fig. 4. Fracture mechanical idealization of the rolling defects as straight inclined edge cracks under the action of membrane and bending stresses.

To calculate the stress intensity factors the thickness W of the wheel disc must be known. With r and W in mm the thickness is approximated by

$$W = 38.2 - 0.447 \cdot r. \tag{5}$$

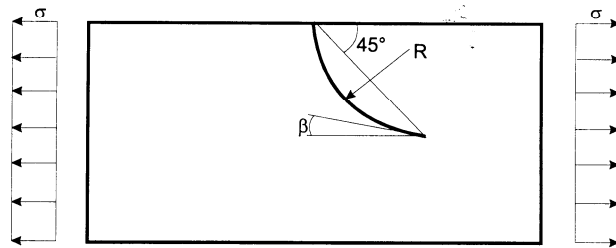


Fig. 5 Fracture mechanical idealization of the rolling defects to investigate the influence of the defect curvature.

Test calculations using the crack model given in Fig. 5 show for crack tip angles $\beta < 45^\circ$ a reduction of the equivalent stress intensity factor compared with the straight crack and for crack tip angles $\beta > 45^\circ$ an increase of up to about 3 per cent over that value of straight cracks. For crack tip directions which tends towards parallel to the surface the model of the straight inclined crack is conservative. For crack tip directions which tends towards transverse to the surface the model of the straight inclined crack is a little bit unsafe.

THRESHOLD VALUES ΔK_{th} OF WHEEL STEEL R1

Only a few published threshold ranges ΔK_{th} of the stress intensity factor for solid wheel steel are known [6]. Most investigations are related to the steels R7 and R9 which are used for wheels with quenched rims [7]. Because of the different carbon content and the heat treatment of the steels investigated before and the old not heat treated steel R1 it is necessary to determine the threshold values ΔK_{th} of the steel R1. The results ΔK_{th} of about 60 tests are given in Fig. 6 against the stress ratio R .

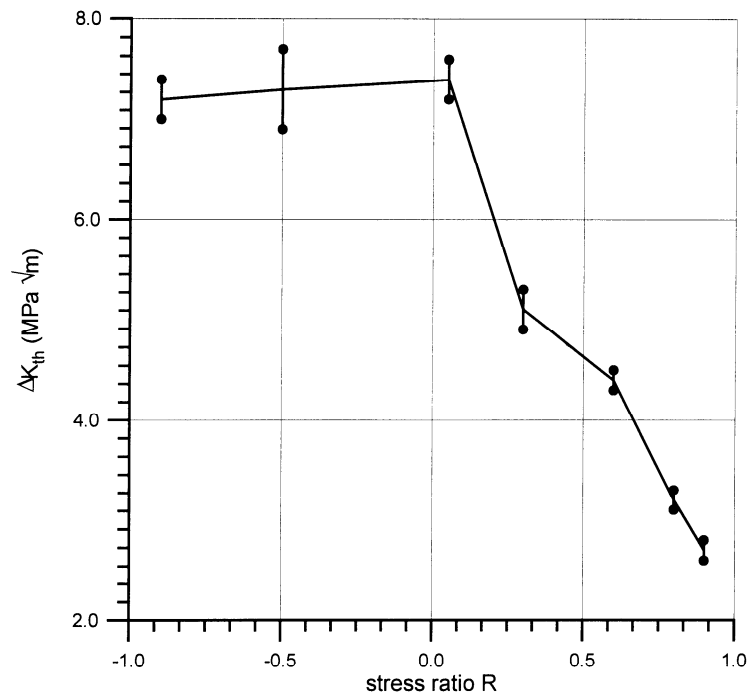


Fig. 6. Mean value and standard deviation of the threshold range ΔK_{th} of the stress intensity factor of the solid wheel steel BV 1 (or R1).

Table 3. Chemical composition of wheel steels [8, 9].

steel	chemical composition in weight per cent				
	C	Si	Mn	P	S
BV1 [8]	---	0.50	1.20	0.05	0.05
R1 [9]	0.48	0.50	0.90	0.035	0.035
R7 [9]	0.52	0.40	0.80	0.035	0.035
R9 [9]	0.60	0.40	0.80	0.035	0.035

MONTE CARLO SIMULATION OF FATIGUE

To compare the material loading with the fracture mechanical properties the stress intensity factors of the mode I and II can be summed up to an equivalent value of the stress intensity factors. Fracture tests [10] and crack growth tests show a good result using the equation

$$K_{I,V} = \frac{1}{2} \cdot \left(K_I + \sqrt{K_I^2 + 6 \cdot K_{II}^2} \right). \quad (6)$$

It can be assumed that the above mentioned equation is also suited for the case of not growing cracks. The fatigue strength condition is then

$$\Delta K_{I,V} = \Delta K_{th} \tag{7}$$

The fracture mechanical calculations of the crack size a at which the cyclic growth begins are performed with random values of the essential properties, parameters, and dimensions. The calculations are repeated 5000 times for the same assumptions to get the probability distribution. As it is unknown how large the membrane stress part and the bending stress part are in the disc the simulation is performed for two extreme assumptions: on the one hand for pure membrane stresses and on the other hand for pure bending stresses (with the same stress values but a calibration factor in the equations for the stress intensity factors which is reduced to 50 per cent compared with that of the membrane stresses).

The Monte Carlo simulation gives three different results:

- For stresses in the pressure range it can be assumed that the cracklike defects cannot grow. (The effect of the small K_{II} will be neglected.) This case won't diminish the safety of the wheels under practical conditions.
- For low stresses in the tension range the threshold crack size can exceed the thickness of the wheel disc. This case likewise won't diminish the safety of the wheels under practical conditions.
- For relatively high stresses in the tension range there exists a threshold crack size between non-growing and growing.

All possible cases are considered appropriate to their probability to get the survival probability of the wheels (Fig. 7). To get a representative value of the non-growing defect size that defect size is selected

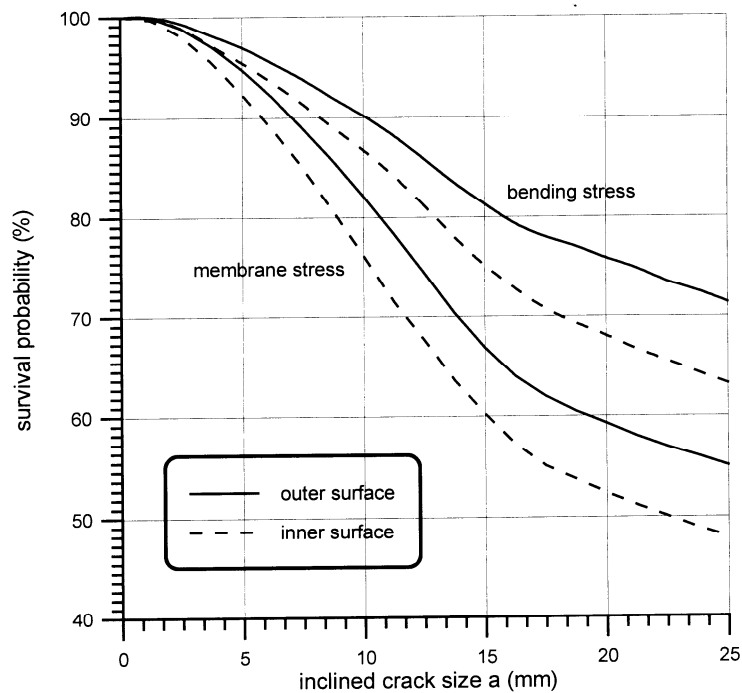


Fig. 7. Probability distribution of the size of non growing defects under service conditions.

from the simulated probability distribution which has a survival probability of 90 per cent. To be independent of the assumptions related to the stress distribution the results of the membrane stress and bending stress calculations are averaged. But this assumption is conservative. More realistic is the assumption of a state of bending stresses. Consequently, on the inner surface of the wheel disc follows

$$a(P_D = 90\%) = \begin{cases} 7,0 \text{ mm} & \text{for the mean of membrane and bending stresses} \\ 8,2 \text{ mm} & \text{for bending stresses} \end{cases} \quad (8)$$

ASSESSMENT OF THE SIMULATION RESULTS

Safety factors to guarantee the durability of cyclic loaded structures which are usually related to the stresses are given in Table 4. For the use in fracture mechanical calculations and assessments, the safety factors must be modified according to the relation

$$S_a = S_\sigma^2 \quad (9)$$

to get safety factors which are related to the crack size.

Table 4. Safety factors S_σ for cyclic loaded structures manufactured of rolled steel [11].

consequences of failure	large	small
<u>large welded structures with not considered residual stresses:</u>		
not periodical NDT	1.9	1.6
periodical NDT	1.7	1.5
<u>other cases of structures:</u>		
not periodical NDT	1.5	1.3
periodical NDT	1.35	1.2

The necessary safety factor to assess the rolling defects has a size of $1,35^2 = 1,82$. The use of the before mentioned safety factor to the representative minimum value of the not growing defects leads to the allowable crack size

$$a_{all} = \frac{a(P_D = 90\%)}{S_a} = \begin{cases} 3,8 \text{ mm} & \text{for the mean of membrane and bending stresses} \\ 4,5 \text{ mm} & \text{for bending stresses.} \end{cases} \quad (11)$$

CONCLUSIONS

The allowable value of the crack size a , which was calculated by means of the LEFM, is not very suitable for the non-destructive testing of the surface of the wheel disc. The length L of the defect on the surface is essentially better suited for the NDT than the inclined crack size a . Starting from the above derived allowable crack size a the allowable value of the crack length L is derived by means of the border line in Fig. 3 to about 40 mm but not smaller than 30 mm. The assessment of rolling defects by means of this allowable defect length does not require the determination of the defect size below the

surface of the wheel disc. The explained method to derive the allowable defect size can likewise be applied to other cyclic loaded structures.

ACKNOWLEDGEMENTS

The investigations presented were initiated by the Deutsche Bundesbahn and sponsored by the Deutsche Forschungsgemeinschaft. The authors wish to thank the DFG for their valuable support and the DB for the permission to publish the results of this investigation.

REFERENCES

1. Börner, U. and Glaser (1995). *Untersuchung von Oberflächenfehlern an Radscheiben*. Brandenburg-Kirchmöser: Deutsche Bahn AG, Forschungs- und Versuchszentrum Kirchmöser, Versuchsbericht 543-001.
2. Edel, K.-O. (1994). *Einschätzung der Dauerfestigkeit von Eisenbahnvollrädern mit Oberflächendefekten im Radscheibenbereich*. Brandenburg an der Havel: Fachhochschule Brandenburg, Forschungsbericht.
3. Wächter, K. and Näbrich, F. (1986). *Berechnung der Temperaturen und thermischen Spannungen für das klotzgebremste Vollrad für 22,5 t Achsfahrmasse*. Dresden: Hochschule für Verkehrswesen Friedrich List, Untersuchungsbericht.
4. Murakami, Y. (ed.) (1987). *Stress intensity factors handbook* (2 vol.), Oxford: Pergamon Press.
5. Bowie, O. L. (1973). *Solutions of plane crack problems by mapping techniques*. In: Sih, G. C. (ed.) *Mechanics of fracture*, vol. 1. Leyden: Noordhoff International Publishing.
6. Edel, K.-O. and Ottlinger, P. (1990). *Fatigue crack growth characteristics of solid wheels*. *Rail International* **21**, 15 - 22.
7. Edel, K.-O. and Schaper, M. (1992). *Fracture mechanics fatigue resistance analysis of the crack-damaged tread of overbraked solid railway wheels*. *Rail International* **23**, 35 - 49.
8. Internationaler Eisenbahnverband (UIC). *Technische Lieferbedingungen für Wagnvollräder*. UIC-Merkblatt 812-3, 2. Ausgabe: 1.1.1963.
9. Internationaler Eisenbahnverband (UIC). *Technische Lieferbedingungen für Vollräder aus gewaltem, unlegiertem Stahl für Triebfahrzeuge und Wagen*. UIC-Merkblatt 812-3, 5. Ausgabe: 1.1.1984.
10. Richard, H. A. (1987). *Praxisnahe Beurteilung von Mixed-Mode-Rißproblemen*. Deutscher Verband für Materialprüfung e.V., Berichte der 19. Sitzung des DVM-Arbeitskreises „Bruchvorgänge“, Freiburg, pp. 357 -370.
11. Hänel, B. and Wirthgen, G. (1993). *Rechnerischer Festigkeitsnachweis für Maschinenbauteile*. Dresden: IMA Materialforschung und Anwendungstechnik GmbH, Abschlußbericht.